

**Supplementary Materials for “Highly Efficient and Robust Catalysts  
for Hydrogen Evolution Reaction by Surface Nano Engineering of  
Metallic Glass”**

Yuqiang Yan<sup>†ab</sup>, Chao Wang<sup>†c</sup>, Zhiyuan Huang<sup>a</sup>, Jianan Fu<sup>a</sup>, Zezhou Lin<sup>a</sup>, Xi Zhang<sup>a</sup>,  
Jiang Ma\*<sup>a</sup>, Jun Shen<sup>a</sup>

<sup>a</sup> College of Mechatronics and Control Engineering, Shenzhen University, Shenzhen  
518060, PR China

<sup>b</sup> Songshan Lake Materials Laboratory, Dongguan 523808, PR China.

<sup>c</sup> Institute of Physics, Chinese Academy of Sciences, Beijing 100190, PR China

**Preparation of Pt@MG NWs.**

The working electrode was prepared in a standard three-electrode single cell system, using MG nanowires as the working electrode, a platinum wire as the counter electrode, and a saturated calomel electrode (SCE) as the reference electrode. The Pt electrode was oxidized from Pt<sup>0</sup> to Pt<sup>2+</sup> dissolved in the electrolyte, and then deposited on the working electrode through electrochemical reduction. Before the platinum ion deposition, the activation of working electrode was cleaned by 50 cycles Cyclic voltammetry (CV) with a scan rate of 100 mV s<sup>-1</sup> from 1.2V to -0.2 V in 0.5 M H<sub>2</sub>SO<sub>4</sub>.

**Electrochemical measurements.**

Electrochemical double-layer capacitance measurements were used to determine the electrochemically active surface areas (ECSA) of the electrocatalysts at non-faradaic overpotentials. The ECSA value was calculated based on the equation of ECSA =  $C_{dl}/C_s$ , where  $C_{dl}$  is the electrochemical double-layer capacitance and  $C_s$  is the specific capacitance. The  $C_s$  for a flat surface was generally found to be in the range of 20 to 60  $\mu$ F cm<sup>-2</sup>. In this work, we used a value of 40  $\mu$ F cm<sup>-2</sup>. A durability test for the Pt@MG NWs catalysts were carried out under static overpotential of 200 mV in 0.5 M H<sub>2</sub>SO<sub>4</sub> for 210 h. The elemental valence of the catalyst was compared after

HER. 5 mg of the 10 wt% Pt/C was dispersed in a 0.9 mL solution of ethanol and 0.1 mL Nafion solution (5%) using ultrasonic treatment to produce with 30min. Then, the 10  $\mu$ L ink was drop-cast onto the GCE, which was then air-dried at room temperature.

XPS analysis.

We performed X-ray photoelectron spectroscopy (XPS) to investigate the surface chemical state of as-obtained Pt@MG NWs (noted as 0 h) and that activated after electrochemical measurements for 210 h. In the high-resolution spectrum of Pt4f (Fig. S9 (a)), Pd3d (Fig. S9 (b)) and Cu2p (Fig. S9 (c)), the peaks at 74.3 and 70.9 eV are indicative of metallic Pt(0) 4f<sub>7/2</sub> and 4f<sub>5/2</sub>, respectively, the peaks at 340.8 and 335.5 eV are assigned to metallic Pd(0) species, the peak at 951.9 and 932.1 eV corresponds to Cu (0) 2p<sub>1/2</sub> and 2p<sub>3/2</sub>, respectively. Owning to the strong dealloying tendency, no Ni2p and P2p peaks are observed in the XPS spectrum.<sup>1</sup> The as-obtained Pt@MG NWs is mainly composed of Pt, Pd, Cu in their metallic forms. There are also minor oxidized Pt and Pd chemical states on the surface from oxidation during sample transfer, the oxidized Cu species is invisible owing to its small fraction. The Pd3d peaks of Pt@MG NWs exhibit an obvious positive shift of 0.5eV towards higher energy compared with pure Pd (3d<sub>3/2</sub> and 3d<sub>5/2</sub> at 340.3 and 335 eV), the shift increases to 0.7 eV after 210 h electrochemical measurement. The Pt4f and Cu2p peaks present a 0.1 eV negative shift and a 0.6eV when compared with pure Pt (4f5/2 and 4f7/2 at 74.4 and 71 eV) and pure Cu (2p3/2 and 2p1/2 at 952.5 and 932.7 eV), suggesting charge transfer from Pd to Pt and Cu. After 210 h electrochemical measurement, the negative shift of Pt4f increase to 0.2 eV, while that of Cu2p peaks remains unchanged. The obviously changed electronic states of Pt, Pd, Cu results from strong electronic coupling among them, which has been observed in other PtPd-based catalysts.<sup>2-4</sup>

The surface composition change can be obtained by using XPS shown in Table S2. In Pt@MG NWs, Ni and P entirely disappears from the surface, and an obvious decrease of Cu content can be identified (Pd:Cu=1:0.23) compared with the nominal composition (Pd:Cu=1:0.75). After 210 h electrochemical tests, the Pt content

increases from 16.75% to 62.63%, indicating that selective dealloying of Pd and Cu happens during the electrochemical testing process. As a result, the surface becomes Pt and Pd abundant, which is crucial to the high catalytical performance.

### Details of calculations.

All density functional theory (DFT) calculations were performed using the Vienna ab initio simulation package (VASP) with the projector augmented wave (PAW) method.<sup>5</sup> The generalized gradient approximation (GGA) with the Perdew, Burke, and Ernzerhof (PBE) functional is chosen for exchange-correlation potential.<sup>6</sup> A cut off the energy of 550 eV was used for the plane-wave basis set and the Monkhorst Pack mesh of  $2 \times 2 \times 1$  k-points was employed for the Brillouin zone integrations ensuring the accuracy of geometry optimizations. The lattice constants and positions of the atoms were optimized until the forces on each atom are less than 0.01 eV/Å, and energy converge is converged to  $10^{-6}$  eV per atom. For  $\text{Pd}_x\text{Pt}_{(64-x)}$  model, a four-layer  $4 \times 4 \times 1$  supercell with a 15 Å vacuum region was considered, the vacuum region was applied to prevent periodic images from interacting with each other, and the lattice parameter in z-direction was fixed. Fixing the underlying mimic substrate (bottom layer) of  $\text{Pd}_x\text{Pt}_{(64-x)}$  model, further geometry optimization was performed so that the geometry was constructed precisely for investigating the realistic reaction process.

The adsorption energy ( $\Delta E_{ad}$ ) describes the energy needed to increase the coverage by an adsorbed hydrogen atom, which is calculated as follows:

$$\Delta E_{ad} = E_{\text{Slab} + nH} - E_{\text{Slab} + (n-1)H} - \frac{1}{2}E_{H_2} \quad (1)$$

where  $E_{\text{Slab} + nH}$  and  $E_{\text{Slab} + (n-1)H}$  represent the total energy of the  $\text{Pd}_x\text{Pt}_{(64-x)}$  system with n and n-1 adsorbed hydrogen atoms on the slab surface, respectively, while  $E_{H_2}$  represents the total energy of a gas phase  $\text{H}_2$  molecule. Gibb's free energy ( $\Delta G$ ) of species adsorbed on a catalyst is considered as a good description of catalytic activity<sup>7</sup>.  $\Delta G$  of the adsorption system is obtained by:

$$\Delta G = \Delta E_{ad} + \Delta E_{ZPE} - T\Delta S \quad (2)$$

$$\Delta E_{ZPE} = E_{ZPE}^{nH} + E_{ZPE}^{(n-1)H} - \frac{1}{2}E_{ZPE}^{H_2} \quad (3)$$

$$\Delta S_H \approx -\frac{1}{2}\Delta S_{H_2}^0 \quad (4)$$

where  $\Delta E_{ad}$ ,  $\Delta E_{ZPE}$ , T and  $\Delta S$  are reaction energy, zero-point energy correction, temperature (300K) and entropy difference, respectively. The calculated  $\Delta E_{ZPE}$  is simplified as 0.11 eV.  $\Delta S_{H_2}^0$  is the entropy of H<sub>2</sub> in the gas phase under standard conditions, and the gas phase value can be obtained from reference ( $S_{H_2}^0 \sim 130 \text{ J}\cdot\text{mol}^{-1}\cdot\text{K}^{-1}$ )<sup>8</sup>. The PH and the potential impact on the free energy change could be neglected.<sup>9</sup>

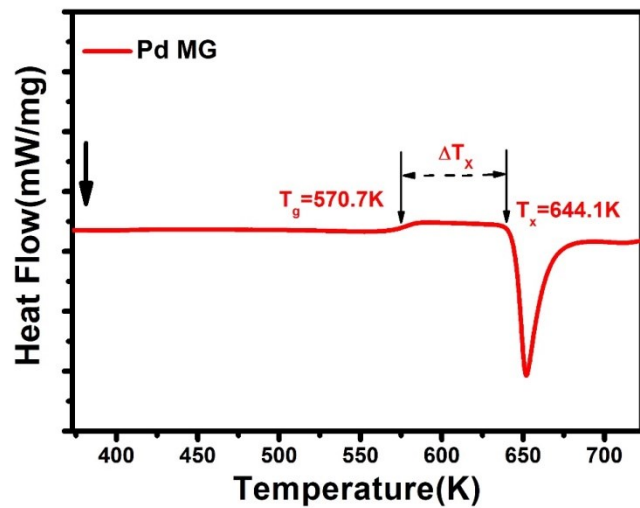


**Fig.S1.** Differential scanning calorimeter (DSC) curve of PdNiCuP MG. The glass transition temperature ( $T_g$ ) and crystallization temperature ( $T_x$ ) are 570.7 K and 644.1 K, respectively. Supercooled liquid region ( $\Delta T_x = T_x - T_g$ ) is calculated to be 73.4K.

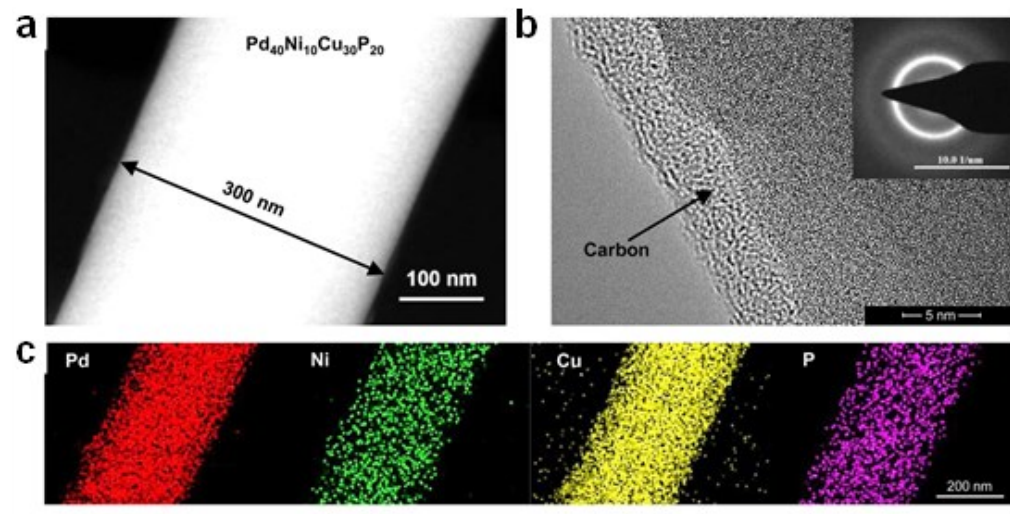


**Fig.S2.** (a) TEM image of a single MG nanowire of  $Pd_{40}Ni_{10}Cu_{30}P_{20}$ . (b) HRTEM image of MG nanowire. The inset shows the selected area electron diffraction pattern. (c) EDX elemental mapping of MG nanowire.

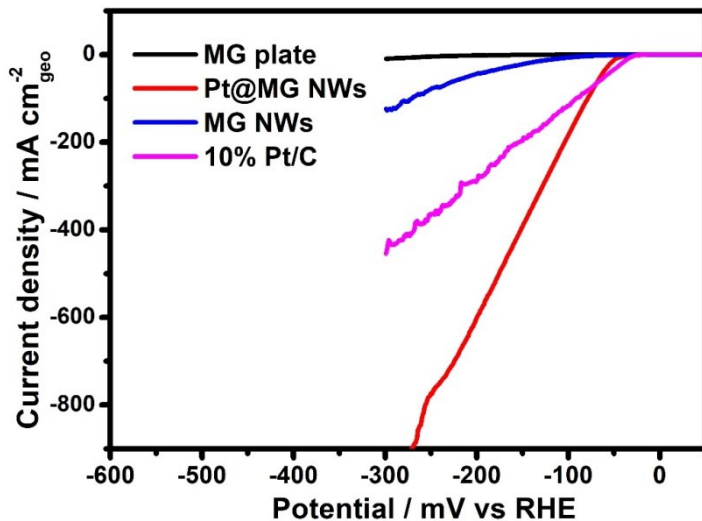


**Fig.S3.** Polarization curves of the MG plate, MG NWs, Pt@MG NWs and Pt/C catalysts with current density normalized to the geometry area in 0.5 M H<sub>2</sub>SO<sub>4</sub> electrolyte at room temperature. The current density normalized to the geometric area of Pt@MG NWs is larger than that of 10% Pt/C with an overpotential larger than 70 mV.

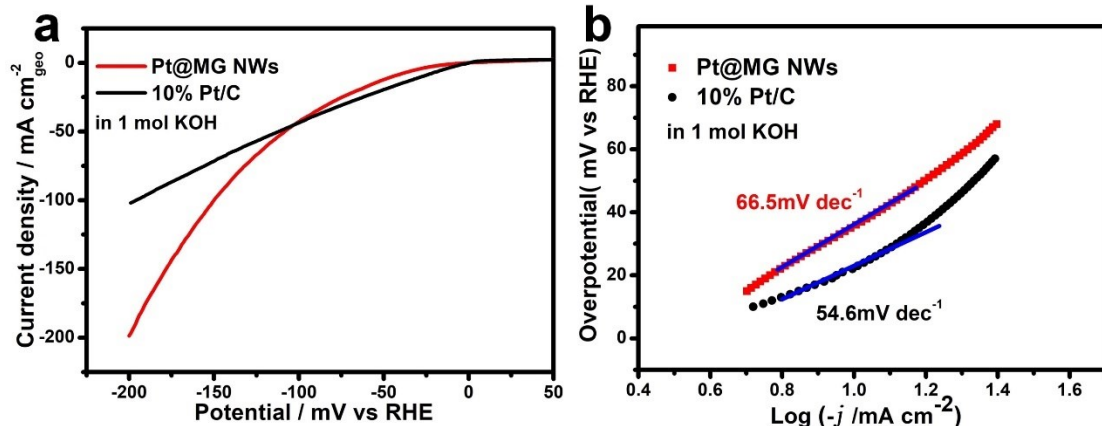


**Fig.S4.** (a) The HER polarization curves for Pt@MG NWs and Pt/C catalysts acquired by linear sweep voltammetry with a scan rate of 2mVs<sup>-1</sup> in 1 M KOH. (b) Corresponding Tafel slope derived from polarization curves.

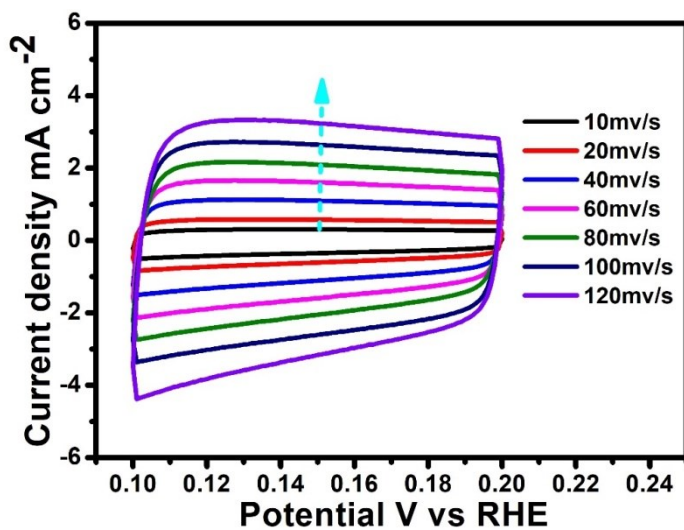


**Fig.S5.** Cyclic voltammograms (CVs) of Pt/C. The CVs were performed at various scan rates (10, 20, 40, 60, 80, 100, and 120  $\text{mV s}^{-1}$ ) from 0.1 to 0.2 V vs RHE.

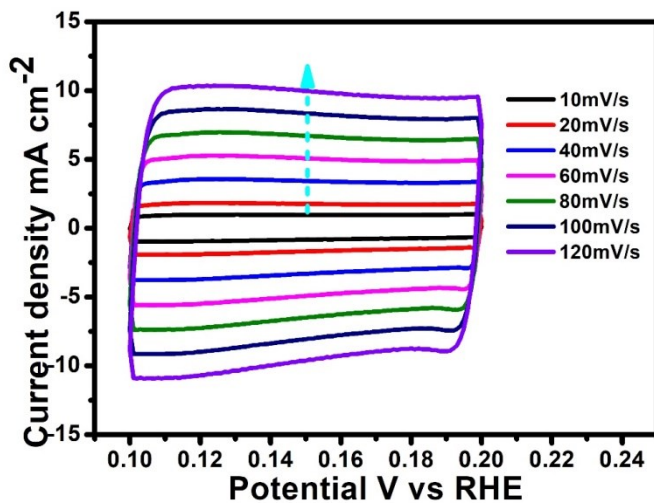


**Fig.S6.** Cyclic voltammograms (CVs) of Pt@MG NWs. The CVs were performed at various scan rates (10, 20, 40, 60, 80, 100, and 120  $\text{mV s}^{-1}$ ) from 0.1 to 0.2V vs RHE.

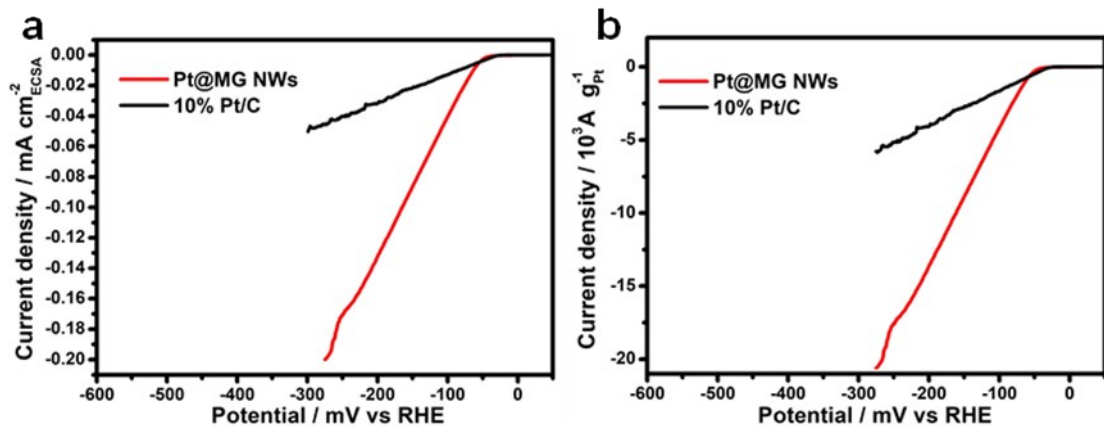


**Fig.S7.** LSV curves of Pt@MG NWs and Pt/C catalysts with current density normalized to the (a) ECSA and (b) mass of Pt in 0.5 M H<sub>2</sub>SO<sub>4</sub> at 2 mV s<sup>-1</sup>.

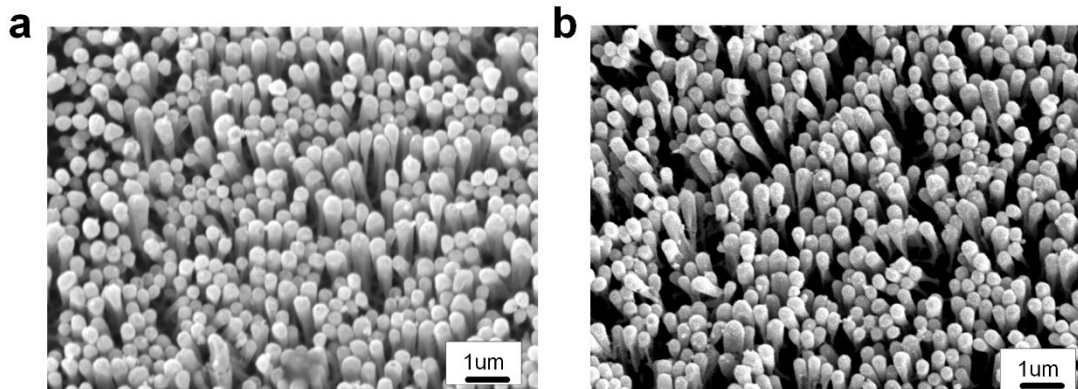


**Fig.S8.** Morphology of Pt@MG NWs (a) before and (b) after 210 hours stability tests.

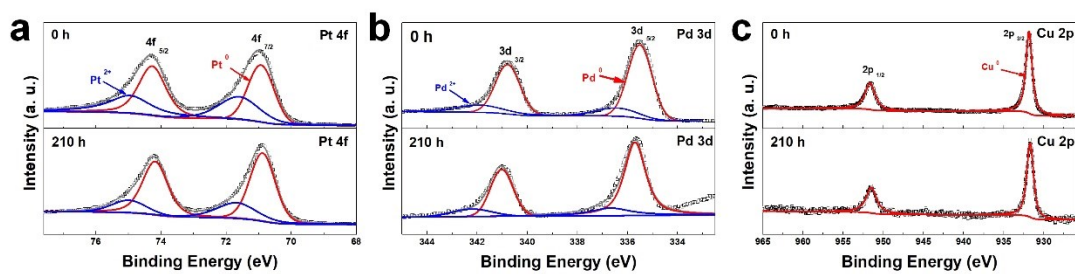


**Fig.S9.** XPS spectra of (a) Pd4f, (b) Pd3d, (c) Cu2p for Pt@MG NWs before and after 210h stability tests in 0.5M H<sub>2</sub>SO<sub>4</sub>.

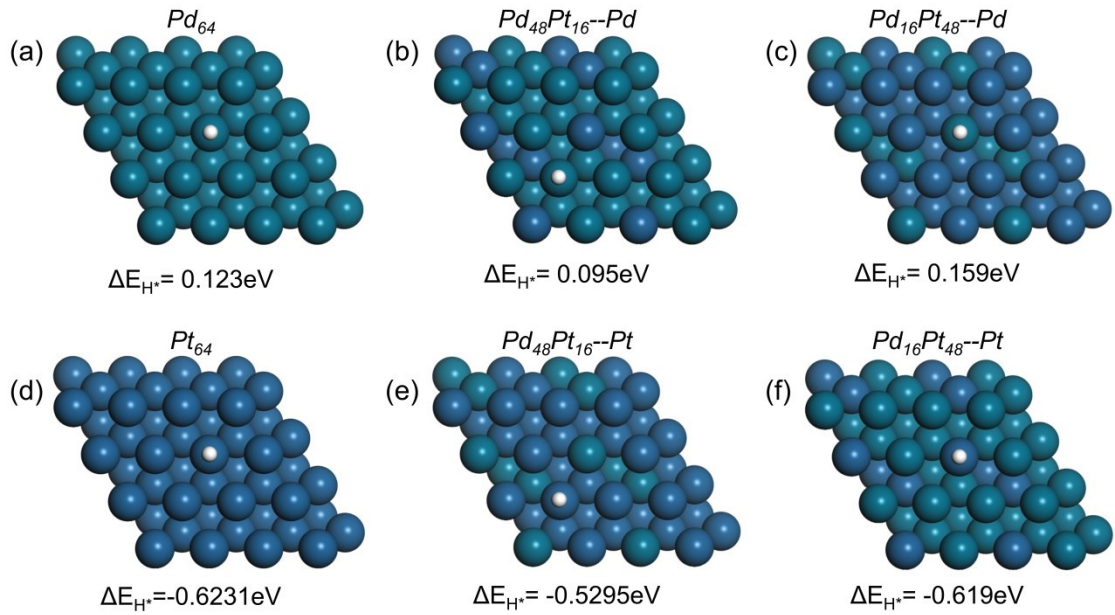


**Fig.S10.** Structural models for  $H^*$  adsorption on (a)  $Pd_{64}$ , (b)  $Pd_{48}Pt_{16}\text{--Pd}$ , (c)  $Pd_{16}Pt_{48}\text{--Pd}$ , (d)  $Pt_{64}$ , (e)  $Pd_{48}Pt_{16}\text{--Pt}$  and (f)  $Pd_{16}Pt_{48}\text{--Pt}$  cluster from the top view.

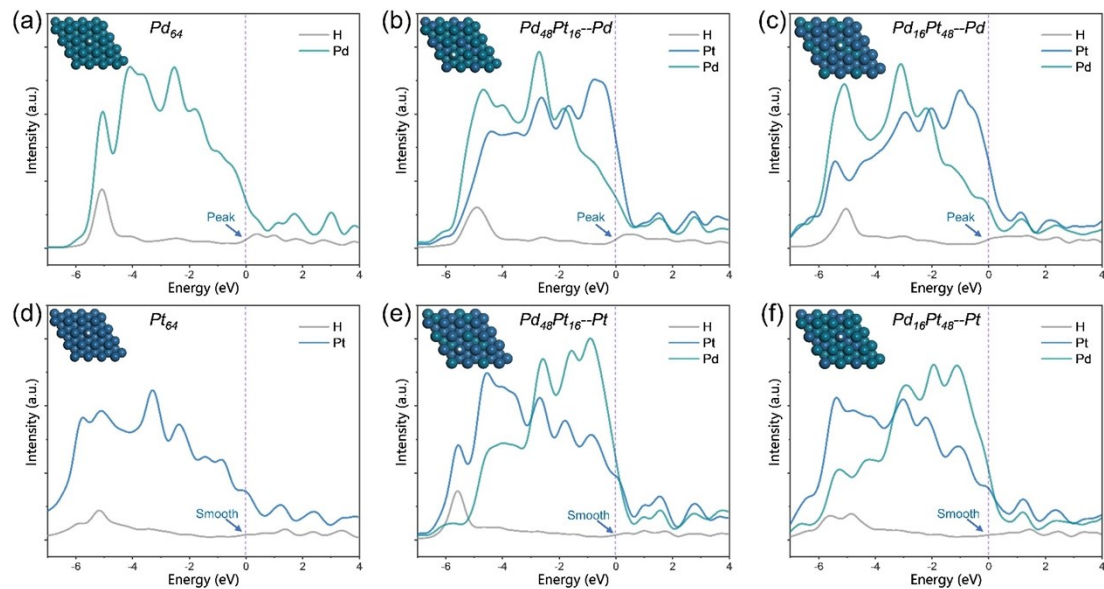


**Fig.S11.** Projected density of states (PDOS) of H and Pd/Pt metal atoms on (a)  $Pd_{64}$ , (b)  $Pd_{48}Pt_{16}\text{--Pd}$ , (c)  $Pd_{16}Pt_{48}\text{--Pd}$ , (d)  $Pt_{64}$ , (e)  $Pd_{48}Pt_{16}\text{--Pt}$  and (f)  $Pd_{16}Pt_{48}\text{--Pt}$  slab.

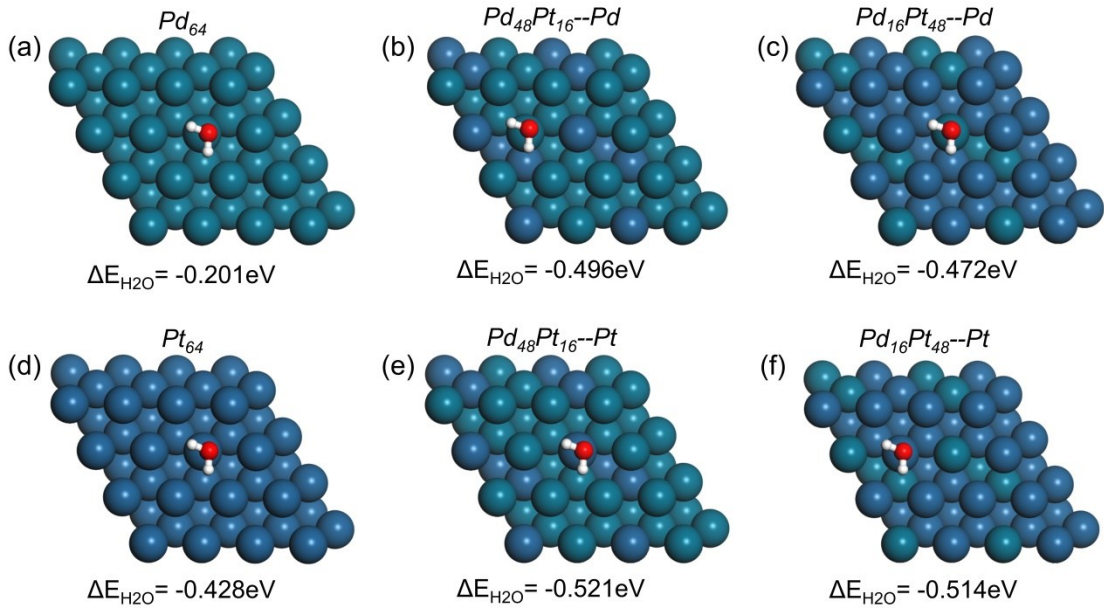


**Fig.S12.** Structural models for  $\text{H}_2\text{O}^*$  adsorption on (a)  $\text{Pd}_{64}$ , (b)  $\text{Pd}_{48}\text{Pt}_{16}\text{--Pd}$ , (c)  $\text{Pd}_{16}\text{Pt}_{48}\text{--Pd}$ , (d)  $\text{Pt}_{64}$ , (e)  $\text{Pd}_{48}\text{Pt}_{16}\text{--Pt}$  and (f)  $\text{Pd}_{16}\text{Pt}_{48}\text{--Pt}$  slab from the top view.

**Table S1.** Calculated adsorption energies  $\Delta E_{H^*}$  and Gibbs free energies  $\Delta G_{H^*}$  of  $\text{Pd}_{64}$ ,  $\text{Pd}_{48}\text{Pt}_{16}\text{--Pd}$ ,  $\text{Pd}_{16}\text{Pt}_{48}\text{--Pd}$ ,  $\text{Pt}_{64}$ ,  $\text{Pd}_{48}\text{Pt}_{16}\text{--Pt}$  and  $\text{Pd}_{16}\text{Pt}_{48}\text{--Pt}$  slab.

Model s	$\text{Pd}_{64}$	$\text{Pt}_{64}$	$\text{Pd}_{48}\text{Pt}_{16}\text{--Pd}$	$\text{Pd}_{48}\text{Pt}_{16}\text{--Pt}$	$\text{Pd}_{16}\text{Pt}_{48}\text{--Pd}$	$\text{Pd}_{16}\text{Pt}_{48}\text{--Pt}$
$E_{\text{slab}+\text{H}^*}$ * (eV)	220024.18 4	46260.032 4	176588.821	176589.44 5	89714.3158	89715.094 3
$E_{\text{slab}}$ (eV)	220008.49 2	46243.593 6	176573.100	176573.10 0	89698.6596	89698.659 6
$\Delta E_{H^*}$ (eV)	0.123	-0.623	0.094	-0.529	0.159	-0.619
$\Delta G_{H^*}$ (eV)	0.435	-0.311	0.406	-0.217	0.471	-0.307

$\Delta G$  is calculated by the equation of  $\Delta G = \Delta E_{ad} + \Delta E_{ZPE} - T\Delta S$

where  $\Delta E_{ad} = E_{Slab + nH} - E_{Slab + (n-1)H} - \frac{1}{2}E_{H_2}$ ,  $\Delta E_{ZPE} = E_{ZPE}^{nH} + E_{ZPE}^{(n-1)H} - \frac{1}{2}E_{ZPE}^{H_2}$ .

**Table S2.** Calculated adsorption energies  $\Delta E_{H2O^*}$  of Pd<sub>64</sub>, Pd<sub>48</sub>Pt<sub>16</sub>--Pd, Pd<sub>16</sub>Pt<sub>48</sub>--Pd, Pt<sub>64</sub>, Pd<sub>48</sub>Pt<sub>16</sub>--Pt and Pd<sub>16</sub>Pt<sub>48</sub>--Pt slab.

Models	Pd <sub>64</sub>	Pt <sub>64</sub>	Pd <sub>48</sub> Pt <sub>16</sub> --Pd	Pd <sub>48</sub> Pt <sub>16</sub> --Pt	Pd <sub>16</sub> Pt <sub>48</sub> --Pd	Pd <sub>16</sub> Pt <sub>48</sub> --Pt
E <sub>slab+H2O</sub> (eV)	220471.75 4	46707.25 2	- 177036.343	- 177036.36 8	-90162.065	90162.107
E <sub>slab+H<sub>2</sub>O(eV)</sub>	220471.55 3	46706.82 4	- 177035.847	177035.84 7	-90161.593	90161.593
$\Delta E_{H2O^*}$ (eV)	-0.201	-0.428	-0.496	-0.521	-0.472	-0.514

$\Delta E_{H2O^*}$  is calculated by the equation of  $\Delta E_{H2O^*} = E_{Slab + H2O^*} - (E_{Slab} + E_{H2O})$

**Table S3.** ICP-MS results of the Pt@MG NWs catalysts

Elements	Volume ml	Dilution Factor	Equipment results mg/L	Concentration mg/kg
Pt	50	1	0.1045	81.1155
Cu	50	50	6.7195	260852.0334
Ni	50	50	2.0615	80026.9268
P	50	50	2.0686	80302.8472
Pd	50	50	14.8986	578361.8865

The mass of the Pt@MG NWs catalyst is 0.24025 g and the geometric area is 0.442 cm<sup>2</sup>. Therefore, the load of Pt in Pt@MG NWs catalysts is 44.09 µg/ cm<sup>-2</sup>.

**Table S4.** XPS results of catalyst surface of MG NWs , Pt@MG NWs 0 h and 210 h.

Sample	Pt	Pd	Cu	Ni	P
	atom %				
MG NWs nominal	-	40	30	10	20

---

**composition**

---

<b>0 h</b>	16.75	67.51	15.74	-	-
<b>210 h</b>	62.63	29.89	7.48	-	-

---

**Table S5.** The Tafel slope and overpotential@10mA cm<sup>-2</sup> of our catalysts were compared with reported HER electrocatalysts.

Catalysts	Overpotential at 10 mA cm <sup>-2</sup> mV vs. RHE	Tafel slope (mVdec <sup>-1</sup> )	Stability	Electrolyte	Refer ences
Pd/Pt-nws	48.5	19.8	10000cv&500h	0.5M H <sub>2</sub> SO <sub>4</sub>	This work
10%Pt/C	36	36.8	10000cv&10h	0.5M H <sub>2</sub> SO <sub>4</sub>	
Ir <sub>25</sub> Ni <sub>33</sub> Ta <sub>42</sub> MG	99	35	1000CV &10h	0.5M H <sub>2</sub> SO <sub>4</sub>	<sup>10</sup>
Pd <sub>40.5</sub> Ni <sub>40.5</sub> Si <sub>4.5</sub> P <sub>14.5</sub> NRAs	MG 63	42.6	40000s	0.5M H <sub>2</sub> SO <sub>4</sub>	
					<sup>11</sup>
Pd <sub>40.5</sub> Ni <sub>40.5</sub> Si <sub>4.5</sub> P <sub>14.5</sub> plate	MG 138	73.6	--	0.5M H <sub>2</sub> SO <sub>4</sub>	
Fe <sub>40</sub> Co <sub>40</sub> P <sub>13</sub> C <sub>7</sub>	118	46	20h	0.5M H <sub>2</sub> SO <sub>4</sub>	<sup>12</sup>
Ni <sub>40</sub> Fe <sub>40</sub> P <sub>20</sub>	193	65	20h	0.5M H <sub>2</sub> SO <sub>4</sub>	<sup>13</sup>
PdCuNi-S MG	48	35	5000cv&24h	0.5M H <sub>2</sub> SO <sub>4</sub>	<sup>14</sup>
Pd <sub>40</sub> Ni <sub>10</sub> Cu <sub>30</sub> P <sub>20</sub> MG	76	58	10000cv&40000s	0.5M H <sub>2</sub> SO <sub>4</sub>	<sup>1</sup>
Pd–Cu–S	58	35	3000cv&48h	0.5M H <sub>2</sub> SO <sub>4</sub>	<sup>15</sup>
Pt SASs/AG	12	29.3	2000cv&24h	0.5M H <sub>2</sub> SO <sub>4</sub>	<sup>16</sup>
Ru SAS@PN	24	38	5000cv&24h	0.5M H <sub>2</sub> SO <sub>4</sub>	<sup>17</sup>
Pt <sub>1</sub> /N-C	19	14.2	20h	0.5M H <sub>2</sub> SO <sub>4</sub>	<sup>18</sup>
ALDPt/NGNs	50	29	1000cv	0.5M H <sub>2</sub> SO <sub>4</sub>	<sup>19</sup>
Co-SAC	230	99	1000cv	0.5M H <sub>2</sub> SO <sub>4</sub>	
Ni-SAC	530	167	--	0.5M H <sub>2</sub> SO <sub>4</sub>	<sup>20</sup>
W-SAC	590	122	--	0.5M H <sub>2</sub> SO <sub>4</sub>	
Pt <sub>1</sub> /MoO <sub>3</sub> -x/C	23.3	29.1	--	0.5M H <sub>2</sub> SO <sub>4</sub>	<sup>21</sup>
A-Ni-C	34	41	4000cv&25h	0.5M H <sub>2</sub> SO <sub>4</sub>	<sup>22</sup>

Pd NP	55	35	10000cv&100h	0.5M H <sub>2</sub> S0 <sub>4</sub>	
					<sup>23</sup>
Pd/C	170	121	48h	0.5M H <sub>2</sub> S0 <sub>4</sub>	
Pt/c	58	33	48h	0.5M H <sub>2</sub> S0 <sub>4</sub>	
CS-PdPt	26	33	1000cv&24h	0.5M H <sub>2</sub> S0 <sub>4</sub>	<sup>24</sup>
rGO-Au48Pd52	130	149		0.5M H <sub>2</sub> S0 <sub>4</sub>	
rGO-Fe48Pd52	250	370	30s	0.5M H <sub>2</sub> S0 <sub>4</sub>	<sup>25</sup>
PdMnCo alloy	39	31	80h	0.5M H <sub>2</sub> S0 <sub>4</sub>	<sup>26</sup>
Pd/C (30 wt%)	96	43	--	0.5M H <sub>2</sub> S0 <sub>4</sub>	
Pt@Pd NFs/rGO	56	39	1000cv&10000s	0.5M H <sub>2</sub> S0 <sub>4</sub>	<sup>27</sup>
Pt <sub>2</sub> Pd/NPG	58	31	4000th&10000s	0.5M H <sub>2</sub> S0 <sub>4</sub>	<sup>28</sup>
PtPd bimetallic	57	36	1000cv&10000s	0.5M H <sub>2</sub> S0 <sub>4</sub>	<sup>29</sup>
PdCo alloy	80	31	10000cv&40000s	0.5M H <sub>2</sub> S0 <sub>4</sub>	<sup>30</sup>
PdCu-Pd	31	35	5000cv&48h	0.5M H <sub>2</sub> S0 <sub>4</sub>	<sup>31</sup>
Ni@Pd	54	54	1000cv	0.5M H <sub>2</sub> S0 <sub>4</sub>	<sup>32</sup>
PdTe	97	90	1000cv&48h	0.5M H <sub>2</sub> S0 <sub>4</sub>	<sup>33</sup>
PdCu <sub>3</sub>	50	34	10000cv	0.5M H <sub>2</sub> S0 <sub>4</sub>	<sup>34</sup>
PdBi <sub>2</sub>	78	63	10000cv	0.5M H <sub>2</sub> S0 <sub>4</sub>	<sup>35</sup>
PdPS	100	46	1000cv	0.5M H <sub>2</sub> S0 <sub>4</sub>	<sup>36</sup>
Pd <sub>17</sub> Se <sub>15</sub>	182	57		0.5M H <sub>2</sub> S0 <sub>4</sub>	
Pd <sub>7</sub> Se <sub>4</sub>	162	56	3000cv	0.5M H <sub>2</sub> S0 <sub>4</sub>	<sup>37</sup>
Pd <sub>4</sub> Se	94	50		0.5M H <sub>2</sub> S0 <sub>4</sub>	
MoO <sub>2</sub> @PC-RGO	64	41	5000cv	0.5M H <sub>2</sub> S0 <sub>4</sub>	<sup>38</sup>
WO <sub>2</sub> @C NWs	58	46	2000cv&10h	0.5M H <sub>2</sub> S0 <sub>4</sub>	<sup>39</sup>
Mo-W18O49 NWs	45	54	5000cv&12h	0.5M H <sub>2</sub> S0 <sub>4</sub>	<sup>40</sup>
WO <sub>2.9</sub>	70	50	1000cv&19000s	0.5M H <sub>2</sub> S0 <sub>4</sub>	<sup>41</sup>
MoN-NC NPs	62	54	3000cv&15h	0.5M H <sub>2</sub> S0 <sub>4</sub>	<sup>42</sup>
WN NA/CC	198	92		0.5M H <sub>2</sub> S0 <sub>4</sub>	<sup>43</sup>
h-MoN @BNCNT	78	46	10000cv&24h	0.5M H <sub>2</sub> S0 <sub>4</sub>	<sup>44</sup>
Ni <sub>3</sub> N NSs	59	60	5000cv&12h	0.5M H <sub>2</sub> S0 <sub>4</sub>	<sup>45</sup>
Fe <sub>2</sub> N/NrGO	94	51	10h	0.5M H <sub>2</sub> S0 <sub>4</sub>	<sup>46</sup>
P-WN/rGO	46	54	5000cv&20h	0.5M H <sub>2</sub> S0 <sub>4</sub>	<sup>47</sup>
CuxNi <sub>4-x</sub> N NSs	52	59	65h	0.5M H <sub>2</sub> S0 <sub>4</sub>	<sup>48</sup>
Pt-MoS <sub>2</sub>	35	25	30h	0.5M H <sub>2</sub> S0 <sub>4</sub>	<sup>49</sup>
MoS <sub>2</sub> film	150	50		0.5M H <sub>2</sub> S0 <sub>4</sub>	<sup>50</sup>
single-layer MoS <sub>2</sub>	185	45	1000cv	0.5M H <sub>2</sub> S0 <sub>4</sub>	<sup>51</sup>
monolayer MoS <sub>2</sub>	226	98	1000cv&9h	0.5M H <sub>2</sub> S0 <sub>4</sub>	<sup>52</sup>

SE-MoS <sub>2</sub>	104	59	24h	0.5M H <sub>2</sub> SO <sub>4</sub>	<sup>53</sup>
P-doped MoS <sub>2</sub> NSs	43	34	5000cv&20h	0.5M H <sub>2</sub> SO <sub>4</sub>	<sup>54</sup>
B-MoSe <sub>2</sub> NSs	84	39	10000cv&20h	0.5M H <sub>2</sub> SO <sub>4</sub>	<sup>55</sup>
FeS <sub>2</sub> -RGO film	139	66	1000cv&10h	0.5M H <sub>2</sub> SO <sub>4</sub>	<sup>56</sup>
MoS <sub>2</sub> /Ni <sub>3</sub> S <sub>2</sub>	98	61	1000cv&50h	0.5M H <sub>2</sub> SO <sub>4</sub>	<sup>57</sup>
CoMoS <sub>3</sub> NRs	143	78	10h	0.5M H <sub>2</sub> SO <sub>4</sub>	<sup>58</sup>
FePSe <sub>3</sub> /NC	70	53	2000cv&24h	0.5M H <sub>2</sub> SO <sub>4</sub>	<sup>59</sup>
Ni-P NSs	98	59	1000cv&160h	0.5M H <sub>2</sub> SO <sub>4</sub>	<sup>60</sup>
Ni <sub>12</sub> P <sub>5</sub> NPs	107	63	1000cv&10000s	0.5M H <sub>2</sub> SO <sub>4</sub>	<sup>61</sup>
CoP NWs	67	51	5000cv&80000s	0.5M H <sub>2</sub> SO <sub>4</sub>	<sup>62</sup>
CoP NPs	75	50	500cv&24h	0.5M H <sub>2</sub> SO <sub>4</sub>	<sup>63</sup>
Co <sub>2</sub> P NPs	95	45		0.5M H <sub>2</sub> SO <sub>4</sub>	
Fe P NRs	58	45	5000cv&20h	0.5M H <sub>2</sub> SO <sub>4</sub>	<sup>64</sup>
FeP <sub>2</sub> NWs	61	37	8h	0.5M H <sub>2</sub> SO <sub>4</sub>	<sup>65</sup>
FeP NPs					
	49	67			
Fe <sub>2</sub> P NPs	83	78	20h	0.5M H <sub>2</sub> SO <sub>4</sub>	<sup>66</sup>
	116	64			
Fe <sub>2</sub> P NPs					
FeP NPs@C	71	52	10000cv	0.5M H <sub>2</sub> SO <sub>4</sub>	<sup>67</sup>
Cu <sub>3</sub> P NWs	143	67	3000cv&25h	0.5M H <sub>2</sub> SO <sub>4</sub>	<sup>68</sup>
MoP NPs	125	54	4000cv&24h	0.5M H <sub>2</sub> SO <sub>4</sub>	<sup>69</sup>
WP NWs	130	69	5000cv&70h	0.5M H <sub>2</sub> SO <sub>4</sub>	<sup>70</sup>
Zn <sub>0.08</sub> Co <sub>0.92</sub> P NSs	39	39	22h	0.5M H <sub>2</sub> SO <sub>4</sub>	<sup>71</sup>
Mo <sub>2</sub> C microparticles	225	56	48h	0.5M H <sub>2</sub> SO <sub>4</sub>	<sup>72</sup>
MoC@C NSs	153	75	1000cv	0.5M H <sub>2</sub> SO <sub>4</sub>	<sup>73</sup>
Mo <sub>2</sub> C@C NSs	78	41	1000cv&12000s	0.5M H <sub>2</sub> SO <sub>4</sub>	<sup>74</sup>
Zn-N-MoC NSs	128	52.1	10h	0.5M H <sub>2</sub> SO <sub>4</sub>	<sup>75</sup>
WC@C NPs	51	49	5h	0.5M H <sub>2</sub> SO <sub>4</sub>	<sup>76</sup>
W <sub>2</sub> C/CNT	50	45	10000cv	0.5M H <sub>2</sub> SO <sub>4</sub>	<sup>77</sup>
N-WC NWs	89	75	20h	0.5M H <sub>2</sub> SO <sub>4</sub>	<sup>78</sup>

Fe-Ni <sub>3</sub> C@C NSs	178	36.5	1000cv	0.5M H <sub>2</sub> S0 <sub>4</sub>	79
Ti <sub>3</sub> C <sub>2</sub> NFs	169	97	12h	0.5M H <sub>2</sub> S0 <sub>4</sub>	80
V <sub>8</sub> C <sub>7</sub> @GC NSs	37	34.5	100h	0.5M H <sub>2</sub> S0 <sub>4</sub>	81
VC@C NSs	98	56	10000cv	0.5M H <sub>2</sub> S0 <sub>4</sub>	82
MoB microparticles	215	55	48h	0.5M H <sub>2</sub> S0 <sub>4</sub>	72
Ni <sub>3</sub> B NPs	79	85	5000cv&24h	0.5M H <sub>2</sub> S0 <sub>4</sub>	83
Co <sub>2</sub> B NPs	328	92.4	5000cv	0.5M H <sub>2</sub> S0 <sub>4</sub>	84
RuB <sub>2</sub> NPs	18	38.9	50h	0.5M H <sub>2</sub> S0 <sub>4</sub>	85
VB <sub>2</sub> microparticles	192	68	2000cv&12h	0.5M H <sub>2</sub> S0 <sub>4</sub>	86
N,S-doped graphene	280	80.5	1000cv	0.5M H <sub>2</sub> S0 <sub>4</sub>	87
EDA-CNTs	150	117	500cv&12h	0.5M H <sub>2</sub> S0 <sub>4</sub>	88
N,P-doped C NWs	163	89	4h	0.5M H <sub>2</sub> S0 <sub>4</sub>	89
3D graphene NWs	107	64	2000cv&5h	0.5M H <sub>2</sub> S0 <sub>4</sub>	90
g-C <sub>3</sub> N <sub>4</sub> /graphene	207	54	54000s	0.5M H <sub>2</sub> S0 <sub>4</sub>	91

### Reference:

- Y. C. Hu, Y. Z. Wang, R. Su, C. R. Cao, F. Li, C. W. Sun, Y. Yang, P. F. Guan, D. W. Ding and Z. L. Wang, *Adv. Mater.*, 2016, **28**, 10293-10297.
- S. Bai, C. Wang, M. Deng, M. Gong, Y. Bai, J. Jiang and Y. Xiong, *Angew. Chem. Int. Ed*, 2014, **53**, 12120-12124.
- C. Hsu, C. Huang, Y. Hao and F. Liu, *Electrochemistry communications*, 2012, **23**, 133-136.
- M. Khan, A. B. Yousaf, M. Chen, C. Wei, X. Wu, N. Huang, Z. Qi and L. Li, *Journal of Power Sources*, 2015, **282**, 520-528.
- G. Kresse and J. Hafner, *Physical Review B*, 1993, **47**, 558.
- J. P. Perdew, K. Burke and M. Ernzerhof, *Phys. Rev. Lett.*, 1996, **77**, 3865.

7. J. Greeley, T. F. Jaramillo, J. Bonde, I. Chorkendorff and J. K. Nørskov, *Nat. Mater.*, 2006, **5**, 909-913.
8. P. Atkins and J. De Paula, *Physical chemistry for the life sciences*, Oxford University Press, USA, 2011.
9. J. K. Nørskov, J. Rossmeisl, A. Logadottir, L. Lindqvist, J. R. Kitchin, T. Bligaard and H. Jónsson, *Journal of Physical Chemistry B*, 2004, **108**, 17886-17892.
10. Z. J. Wang, M. X. Li, J. H. Yu, X. B. Ge, Y. H. Liu and W. H. Wang, *Adv Mater*, 2020, **32**, e1906384.
11. Z. J. Wang, M. X. Li, J. H. Yu, X. B. Ge, Y. H. Liu and W. H. Wang, *Adv. Mater*, 2020, **32**, 1906384.
12. F. Zhang, J. Wu, W. Jiang, Q. Hu and B. Zhang, *ACS applied materials & interfaces*, 2017, **9**, 31340-31344.
13. Y. Tan, F. Zhu, H. Wang, Y. Tian, A. Hirata, T. Fujita and M. Chen, *Advanced Materials Interfaces*, 2017, **4**, 1601086.
14. X. Yang, W. Xu, S. Cao, S. Zhu, Y. Liang, Z. Cui, X. Yang, Z. Li, S. Wu, A. Inoue and L. Chen, *Appl. Catal. B*, 2019, **246**, 156-165.
15. W. Xu, S. Zhu, Y. Liang, Z. Cui, X. Yang, A. Inoue and H. Wang, *J. Mater. Chem. A*, 2017, **5**, 18793-18800.
16. S. Ye, F. Luo, Q. Zhang, P. Zhang, T. Xu, Q. Wang, D. He, L. Guo, Y. Zhang, C. He, X. Ouyang, M. Gu, J. Liu and X. Sun, *Energy Environ. Sci*, 2019, **12**, 1000-1007.
17. J. Yang, B. Chen, X. Liu, W. Liu, Z. Li, J. Dong, W. Chen, W. Yan, T. Yao, X. Duan, Y. Wu and Y. Li, *Angew Chem Int Ed Engl*, 2018, **57**, 9495-9500.
18. S. Fang, X. Zhu, X. Liu, J. Gu, W. Liu, D. Wang, W. Zhang, Y. Lin, J. Lu, S. Wei, Y. Li and T. Yao, *Nat. Commun*, 2020, **11**, 1029.
19. N. Cheng, S. Stambula, D. Wang, M. N. Banis, J. Liu, A. Riese, B. Xiao, R. Li, T.-K. Sham and L.-M. Liu, *Nat. Commun*, 2016, **7**, 1-9.
20. M. D. Hossain, Z. Liu, M. Zhuang, X. Yan, G. L. Xu, C. A. Gadre, A. Tyagi, I. H. Abidi, C. J. Sun and H. Wong, *Adv. Energy Mater*, 2019, **9**, 1803689.
21. W. Liu, Q. Xu, P. Yan, J. Chen, Y. Du, S. Chu and J. Wang, *ChemCatChem*, 2018, **10**, 946-950.
22. L. Fan, P. F. Liu, X. Yan, L. Gu, Z. Z. Yang, H. G. Yang, S. Qiu and X. Yao, *Nat. Commun*, 2016, **7**, 1-7.

23. T. Bhowmik, M. K. Kundu and S. Barman, *ACS Catal*, 2016, **6**, 1929-1941.
24. B. T. Jebaslinhepzybai, N. Prabu and M. Sasidharan, *Int. J. Hydrogen Energy*, 2020.
25. J. Cardoso, L. Amaral, Ö. Metin, D. Cardoso, M. Sevim, T. Sener, C. Sequeira and D. Santos, *Int. J. Hydrogen Energy*, 2017, **42**, 3916-3925.
26. R. Zhang, Z. Sun, R. Feng, Z. Lin, H. Liu, M. Li, Y. Yang, R. Shi, W. Zhang and Q. Chen, *ACS applied materials & interfaces*, 2017, **9**, 38419-38427.
27. X.-X. Lin, A.-J. Wang, K.-M. Fang, J. Yuan and J.-J. Feng, *ACS Sustainable Chemistry & Engineering*, 2017, **5**, 8675-8683.
28. X. Zhong, Y. Qin, X. Chen, W. Xu, G. Zhuang, X. Li and J. Wang, *Carbon*, 2017, **114**, 740-748.
29. Z.-Z. Yang, X.-X. Lin, X.-F. Zhang, A.-J. Wang, X.-Y. Zhu and J.-J. Feng, *Journal of Alloys and Compounds*, 2018, **735**, 2123-2132.
30. J. Chen, G. Xia, P. Jiang, Y. Yang, R. Li, R. Shi, J. Su and Q. Chen, *ACS applied materials & interfaces*, 2016, **8**, 13378-13383.
31. J. Li, F. Li, S.-X. Guo, J. Zhang and J. Ma, *ACS applied materials & interfaces*, 2017, **9**, 8151-8160.
32. J. Li, P. Zhou, F. Li, R. Ren, Y. Liu, J. Niu, J. Ma, X. Zhang, M. Tian and J. Jin, *J. Mater. Chem. A*, 2015, **3**, 11261-11268.
33. L. Jiao, F. Li, X. Li, R. Ren, J. Li, X. Zhou, J. Jin and R. Li, *Nanoscale*, 2015, **7**, 18441-18445.
34. R. Jana, A. Bhim, P. Bothra, S. K. Pati and S. C. Peter, *ChemSusChem*, 2016, **9**, 2922-2927.
35. S. Sarkar, U. Subbarao and S. C. Peter, *J. Mater. Chem. A*, 2017, **5**, 15950-15960.
36. S. Sarkar and S. Sampath, *Chem. Commun*, 2014, **50**, 7359-7362.
37. S. Kukunuri, P. M. Austeria and S. Sampath, *Chem. Commun*, 2016, **52**, 206-209.
38. Y. J. Tang, M. R. Gao, C. H. Liu, S. L. Li, H. L. Jiang, Y. Q. Lan, M. Han and S. H. Yu, *Angew. Chem. Int. Ed*, 2015, **54**, 12928-12932.
39. R. Wu, J. Zhang, Y. Shi, D. Liu and B. Zhang, *J. Am. Chem. Soc*, 2015, **137**, 6983-6986.
40. X. Zhong, Y. Sun, X. Chen, G. Zhuang, X. Li and J. G. Wang, *Adv. Funct. Mater*, 2016, **26**, 5778-5786.

41. Y. H. Li, P. F. Liu, L. F. Pan, H. F. Wang, Z. Z. Yang, L. R. Zheng, P. Hu, H. J. Zhao, L. Gu and H. G. Yang, *Nat. Commun.*, 2015, **6**, 8064.
42. Y. Zhu, G. Chen, X. Xu, G. Yang, M. Liu and Z. Shao, *ACS Catal.*, 2017, **7**, 3540-3547.
43. J. Shi, Z. Pu, Q. Liu, A. M. Asiri, J. Hu and X. Sun, *Electrochim. Acta*, 2015, **154**, 345-351.
44. J. Miao, Z. Lang, X. Zhang, W. Kong, O. Peng, Y. Yang, S. Wang, J. Cheng, T. He and A. Amini, *Adv. Funct. Mater.*, 2019, **29**, 1805893.
45. D. Gao, J. Zhang, T. Wang, W. Xiao, K. Tao, D. Xue and J. Ding, *J. Mater. Chem. A*, 2016, **4**, 17363-17369.
46. Y. Zhang, Y. Xie, Y. Zhou, X. Wang and K. Pan, *Journal of Materials Research*, 2017, **32**, 1770-1776.
47. H. Yan, C. Tian, L. Wang, A. Wu, M. Meng, L. Zhao and H. Fu, *Angew. Chem. Int. Ed.*, 2015, **54**, 6325-6329.
48. Y. Ma, Z. He, Z. Wu, B. Zhang, Y. Zhang, S. Ding and C. Xiao, *J. Mater. Chem. A*, 2017, **5**, 24850-24858.
49. Z. Chen, K. Leng, X. Zhao, S. Malkhandi, W. Tang, B. Tian, L. Dong, L. Zheng, M. Lin and B. S. Yeo, *Nat. Commun.*, 2017, **8**, 1-9.
50. J. Kibsgaard, Z. Chen, B. N. Reinecke and T. F. Jaramillo, *Nat. Mater.*, 2012, **11**, 963.
51. Y. Wan, Z. Zhang, X. Xu, Z. Zhang, P. Li, X. Fang, K. Zhang, K. Yuan, K. Liu, G. Ran, Y. Li, Y. Ye and L. Dai, *Nano Energy*, 2018, **51**, 786-792.
52. Y. Tan, P. Liu, L. Chen, W. Cong, Y. Ito, J. Han, X. Guo, Z. Tang, T. Fujita and A. Hirata, *Adv. Mater.*, 2014, **26**, 8023-8028.
53. J. Hu, B. Huang, C. Zhang, Z. Wang, Y. An, D. Zhou, H. Lin, M. K. Leung and S. Yang, *Energy Environ. Sci.*, 2017, **10**, 593-603.
54. P. Liu, J. Zhu, J. Zhang, P. Xi, K. Tao, D. Gao and D. Xue, *ACS Energy Letters*, 2017, **2**, 745-752.
55. D. Gao, B. Xia, C. Zhu, Y. Du, P. Xi, D. Xue, J. Ding and J. Wang, *J. Mater. Chem. A*, 2018, **6**, 510-515.
56. Y. Chen, S. Xu, Y. Li, R. J. Jacob, Y. Kuang, B. Liu, Y. Wang, G. Pastel, L. G. Salamanca-Riba and M. R. Zachariah, *Adv. Energy Mater.*, 2017, **7**, 1700482.
57. Y. Yang, K. Zhang, H. Lin, X. Li, H. C. Chan, L. Yang and Q. Gao, *ACS Catal.*, 2017, **7**, 2357-2366.

58. J. Guo, X. Zhang, Y. Sun, L. Tang and X. Zhang, *J. Mater. Chem. A*, 2017, **5**, 11309-11315.
59. J. Yu, W.-J. Li, H. Zhang, F. Zhou, R. Li, C.-Y. Xu, L. Zhou, H. Zhong and J. Wang, *Nano Energy*, 2019, **57**, 222-229.
60. X. Wang, W. Li, D. Xiong, D. Y. Petrovykh and L. Liu, *Adv. Funct. Mater.*, 2016, **26**, 4067-4077.
61. Z. Huang, Z. Chen, Z. Chen, C. Lv, H. Meng and C. Zhang, *ACS nano*, 2014, **8**, 8121-8129.
62. J. Tian, Q. Liu, A. M. Asiri and X. Sun, *J. Am. Chem. Soc*, 2014, **136**, 7587-7590.
63. J. F. Callejas, C. G. Read, E. J. Popczun, J. M. McEnaney and R. E. Schaak, *Chem. Mater.*, 2015, **27**, 3769-3774.
64. Y. Liang, Q. Liu, A. M. Asiri, X. Sun and Y. Luo, *ACS Catal.*, 2014, **4**, 4065-4069.
65. C. Y. Son, I. H. Kwak, Y. R. Lim and J. Park, *Chem. Commun.*, 2016, **52**, 2819-2822.
66. D. E. Schipper, Z. Zhao, H. Thirumalai, A. P. Leitner, S. L. Donaldson, A. Kumar, F. Qin, Z. Wang, L. C. Grabow and J. Bao, *Chem. Mater.*, 2018, **30**, 3588-3598.
67. D. Y. Chung, S. W. Jun, G. Yoon, H. Kim, J. M. Yoo, K.-S. Lee, T. Kim, H. Shin, A. K. Sinha and S. G. Kwon, *J. Am. Chem. Soc*, 2017, **139**, 6669-6674.
68. J. Tian, Q. Liu, N. Cheng, A. M. Asiri and X. Sun, *Angew. Chem. Int. Ed*, 2014, **53**, 9577-9581.
69. Z. Xing, Q. Liu, A. M. Asiri and X. Sun, *Adv. Mater.*, 2014, **26**, 5702-5707.
70. Z. Pu, Q. Liu, A. M. Asiri and X. Sun, *ACS applied materials & interfaces*, 2014, **6**, 21874-21879.
71. T. Liu, D. Liu, F. Qu, D. Wang, L. Zhang, R. Ge, S. Hao, Y. Ma, G. Du and A. M. Asiri, *Adv. Energy Mater.*, 2017, **7**, 1700020.
72. H. Vrubel and X. Hu, *Angewandte Chemie International Edition*, 2012, **51**, 12703-12706.
73. Y. Yang, M. Luo, Y. Xing, S. Wang, W. Zhang, F. Lv, Y. Li, Y. Zhang, W. Wang and S. Guo, *Adv. Mater.*, 2018, **30**, 1706085.
74. G. Zhou, Q. Yang, X. Guo, Y. Chen, L. Xu, D. Sun and Y. Tang, *Int. J. Hydrogen Energy*, 2018, **43**, 9326-9333.

75. Q. Cao, L. Zhao, A. Wang, L. Yang, L. Lai, Z.-L. Wang, J. Kim, W. Zhou, Y. Yamauchi and J. Lin, *Nanoscale*, 2019, **11**, 1700-1709.
76. Y.-T. Xu, X. Xiao, Z.-M. Ye, S. Zhao, R. Shen, C.-T. He, J.-P. Zhang, Y. Li and X.-M. Chen, *J. Am. Chem. Soc.*, 2017, **139**, 5285-5288.
77. Q. Gong, Y. Wang, Q. Hu, J. Zhou, R. Feng, P. N. Duchesne, P. Zhang, F. Chen, N. Han and Y. Li, *Nat. Commun.*, 2016, **7**, 1-8.
78. N. Han, K. R. Yang, Z. Lu, Y. Li, W. Xu, T. Gao, Z. Cai, Y. Zhang, V. S. Batista and W. Liu, *Nat. Commun.*, 2018, **9**, 1-10.
79. H. Fan, H. Yu, Y. Zhang, Y. Zheng, Y. Luo, Z. Dai, B. Li, Y. Zong and Q. Yan, *Angew. Chem. Int. Ed.*, 2017, **56**, 12566-12570.
80. W. Yuan, L. Cheng, Y. An, H. Wu, N. Yao, X. Fan and X. Guo, *ACS Sustainable Chemistry & Engineering*, 2018, **6**, 8976-8982.
81. H. Xu, J. Wan, H. Zhang, L. Fang, L. Liu, Z. Huang, J. Li, X. Gu and Y. Wang, *Adv. Energy Mater.*, 2018, **8**, 1800575.
82. X. Peng, L. Hu, L. Wang, X. Zhang, J. Fu, K. Huo, L. Y. S. Lee, K.-Y. Wong and P. K. Chu, *Nano Energy*, 2016, **26**, 603-609.
83. X. Xu, Y. Deng, M. Gu, B. Sun, Z. Liang, Y. Xue, Y. Guo, J. Tian and H. Cui, *Applied Surface Science*, 2019, **470**, 591-595.
84. J. Masa, P. Weide, D. Peeters, I. Sinev, W. Xia, Z. Sun, C. Somsen, M. Muhler and W. Schuhmann, *Adv. Energy Mater.*, 2016, **6**, 1502313.
85. Q. Li, X. Zou, X. Ai, H. Chen, L. Sun and X. Zou, *Adv. Energy Mater.*, 2019, **9**, 1803369.
86. P. R. Jothi, Y. Zhang, K. Yubuta, D. Culver, M. Conley and B. Fokwa, *ACS Applied Energy Materials*, 2018, **2**, 176-181.
87. Y. Ito, W. Cong, T. Fujita, Z. Tang and M. Chen, *Angew. Chem. Int. Ed.*, 2015, **54**, 2131-2136.
88. T. Li, D. Tang, Z. Cui, B. Cai, D. Li, Q. Chen and C. Li, *Electrocatalysis*, 2018, **9**, 573-581.
89. J. Zhang, L. Qu, G. Shi, J. Liu, J. Chen and L. Dai, *Angew. Chem. Int. Ed.*, 2016, **55**, 2230-2234.
90. H. Wang, X. B. Li, L. Gao, H. L. Wu, J. Yang, L. Cai, T. B. Ma, C. H. Tung, L. Z. Wu and G. Yu, *Angewandte Chemie*, 2018, **130**, 198-203.
91. Y. Zhao, F. Zhao, X. Wang, C. Xu, Z. Zhang, G. Shi and L. Qu, *Angew. Chem. Int. Ed.*, 2014, **53**, 13934-13939.